Water Dependent Properties of Cutinase in Nonaqueous Solvents: A Computational Study of Enantioselectivity

Nuno M. Micaelo, Vitor H. Teixeira, António M. Baptista, and Cláudio M. Soares
Instituto de Tecnologia Química e Biológica, Universidade Nova de Lisboa, 2781-901 Oeiras, Portugal

ABSTRACT The catalytic properties of enzymes in nonaqueous solvents are known to be dependent on the nature of the solvent. Here we present a molecular modeling study of the enantioselective properties of the enzyme cutinase in hexane under varying hydration conditions. Previous simulation studies have shown that for this model enzyme in hexane, the structural and dynamical properties are affected by the amount of water associated with the protein, being more similar to the aqueous simulation at 5–10% of water content. The implications of the hydration levels on the enzyme resolution of (R,S)-1-phenylethanol and (R,S)-2-phenyl-1-propanol are investigated using free energy calculations of the tetrahedral intermediate (TI) model. With this model system we show that the enzyme enantioselective properties are under the control of the amount of water present in the organic media. Maximum enantioselectivity is achieved at 10% water content. The stabilizing effects of the catalytic histidine on the TI are evaluated at different water contents and shown to be correlated. The correlation between the amount of water present in the media and the structural, dynamical, and thermodynamic properties of the enzyme are examined as well as the active site discriminative power.

INTRODUCTION

Organic solvents have been widely used as solvents in biocatalytic reactions due to all known advantages that such media offer (1). Besides the interest it arouses in biotechnology, nonaqueous enzymology has also provided insights into the fundamental events in catalysis. Such knowledge is not only restricted to the situation in nonaqueous solvents since the key features governing the selectivity and activity of enzymes in such media can be extended and correlated with the same events occurring in aqueous solutions.

It has been recognized that water in nonaqueous systems has an important role in controlling the catalytic properties of enzymes (2–4). Due to the low miscibility of water in low dielectric solvents, water and ions are mostly associated with the protein surface, acting as a molecular lubricant (4). Therefore, the quantity of water available in nonaqueous solvents is considered one of the factors that control the catalytic properties of enzymes, being thus the subject of extensive research. The amount of water for optimum activity has been, in some cases, successfully correlated with the nature of the solvent, with high catalytic activity being achieved in a specific range of water activity (a_w) (5).

The mechanisms involved in the process of enzyme recognition of enantiomeric substrates and the way nonaqueous solvents are able to increase or decrease the enzyme enantioselectivity are still a matter of research. From a theoretical point of view, there is no fundamental difference between the major factors that can account for the efficient catalytic properties of enzymes and its selectivity in aqueous or nonaqueous solvents. Extensive computational research on aqueous enzyme catalysis has been able to clarify most of the leading events in the catalytic process of the enzymes (see Warshel et al. (6) and Kollman et al. (7) as examples), but there are still questions open to discussion. It is known that the catalytic efficiency of enzymes relies on a preorganized active site, providing an electrostatic stabilization of the transition state (TS), as has been emphasized by Warshel and co-workers (8). The relative importance of the dynamical effects of the enzyme, the entropic contributions, and other aspects has been a subject of controversy (for recent reviews see Cleland et al. (9), Cannon and Benkovic (10), and Warshel (11)). These findings are true for reactions occurring in aqueous solvents but also for nonaqueous enzymology. In the latter, the stabilization of the TS by the enzyme has also to occur, and other aspects have to be taken into consideration, such as the nature of the nonaqueous solvent used and how it should be incorporated into the theoretical framework. Several theories concerning the effects of organic solvents in the process of enzyme-substrate recognition have been proposed. It has been argued that the enzyme selectivity could be altered by the organic solvent by means of a direct interaction with the enzyme active site (12–14). It was also suggested that the solvent could alter the enzyme conformation, affecting the enzyme substrate specificity (15). Other authors propose that the solvent dependence of enzymatic selectivity could be determined from the thermodynamics of substrate solvation (16,17).

Lipases and proteases have been widely used in the study of enzyme activity in nonaqueous solvents. Several experiments have been done in pursuit of the relation between the solvent nature and enzyme activity and selectivity, especially enantioselectivity. Indeed, a direct correlation was often found between the water content and the enantioselective properties of enzymes in organic solvents. Experimentally,

Submitted March 21, 2005, and accepted for publication May 16, 2005.

Address reprint requests to Dr. Cláudio Soares, Tel.: 351-21-4469610; Fax: 351-21-4433644; E-mail: claudio@itqb.unl.pt.

0006-3495/05/08/999/10 $2.00
doi: 10.1529/biophysj.105.063297

Fitzpatrick and Klibanov (15) have shown that, in the transesterification reaction between vinyl butyrate and homologous chiral alcohols in dioxane using subtilisin Carlsberg, the increase of water content in the media was responsible for a decrease in enzyme enantioselectivity. Pepin and Lortie (18) also reported that for Novozym 435, low water activities induced higher enantioselectivity of (R,S)-ibuprofen with dodecanol in octane. However, Person and others (19) reported a direct correlation between enzyme enantioselectivity and water content for the hydroxylnitrile lyases and no significant correlation for the lipases except for the *Candida rugosa* lipase. The role of water in nonaqueous media has been, therefore, a subject of long debate. With the control of the amount of water in such media, the properties of the solvent and, consequently, the molecular properties of the enzymes can be modified and tuned for a specific purpose. This is, apart from point mutations studies, a valuable tool to alter the enzyme selectivity and catalytic properties.

Early theoretical studies on enzyme enantioselectivity (20,21) involved R/S enantiomeric substrates. Some of the molecular details involved in the serine protease α-chymotrypsin, such as hydrogen bonds and stabilization of the tetrahedral intermediate (TI), were described by these molecular modeling studies. Nonaqueous enzymology has provided interesting new case studies for the computational study of enzyme enantioselectivity. Wescott and others (16) addressed the solvent dependence of enzymatic selectivity based on substrate solvation, and later on, vacuum molecular mechanics with continuum electrostatics provided a first glimpse of the solvent-enzyme-substrate interaction on a hydrophobic environment (22). More recently, force field potential energies, energy-based subsets, and structural information were used to estimate the relative free energy of stabilization between the R and S substrate enantiomers in lipases (23,24). Results show a good prediction of the fast-reacting enantiomer and the structural strain involved in enantioselectivity. A more detailed description of the steric and electrostatic complementarity of the serine protease subtilisin in dimethyl formamide has been done by Colombo (25) using quantum mechanics/molecular mechanics (QM/MM) and free energy perturbation methods.

Recent protein modeling studies have tackled this question from the basis of the structural and dynamical behavior of enzymes (26). For cutinase in hexane, it was shown that the Cα root mean-square (rms) deviation is clearly correlated with the amount of water. The correlation profile shows a bell-shapedlike behavior with enzyme structural properties more nativelike within the 5–10% water (w/w (water weight/protein weight)) content. Additionally, the dynamical behavior of the enzyme in the 5–10% water range is similar to what is found in water simulations. This study will be focused on the factors involved in the mechanism of cutinase enantioselectivity toward substrates with chiral centers. This will be accomplished through the evaluation of the relative stability of the corresponding R/S TI. We also investigate how the enzyme structural, dynamical, and thermodynamic properties are affected by the different amounts of water present in the organic media and how this affects the discriminative power of the enzyme.

MATERIAL AND METHODS

Molecular dynamics/mechanics simulations

The general simulation methodology applied in the molecular dynamics/molecular mechanics (MD/MM) simulations of cutinase in hexane with increasing amounts of water was similar to the one we applied in a previous work (26). The 1.0 Å cutinase structure of Longhi was used (27), and the protonated state of charged residues was estimated using a methodology previously described (28). The selection of counterion positions and the different amounts of water hydrating the enzyme was done as explained in detail elsewhere (26). MD/MM simulations were performed with the GROMACS package (29,30) using the GROMOS96 force field (31,32). Bond lengths of the solute and hexane molecules were constrained with LINCS (33) and the ones of water with SETTLE (34). Nonbonded interactions were calculated using a twin-range method (32) with short and long range cutoffs of 8 Å and 14 Å, respectively. The simple point change water model (35) was used in aqueous and in nonaqueous simulations. A reaction field correction for electrostatic interactions (36,37) was applied, considering a dielectric of 54 for simple point change water (38). Hexane was modeled as a flexible united atom model using the GROMOS96 alkane parameters. The simulations were made in the isothermal-isobaric ensemble (NPT). The protein, ions, hexane, and water were coupled to four separated heat baths (39) with temperature coupling constants of 0.1 ps and reference temperatures of 300 K. The pressure control (39) was implemented with a reference pressure of 1 atm and a relaxation time of 0.5 ps and 1.3 ps for water or hexane/water solvents simulations, respectively. The water percentages (w/w) used to hydrate the enzyme were 0%, 2.5%, 5%, 7.5%, 10%, 15%, and 25%. Five replicate MD runs of 7 ns were performed for each system. For the fully hydrated equivalent system in water, three replicate MD runs of 5 ns were done.

Substrate modeling

Two chiral (R,S) substrates of 1-phenylethanol (1PE) and 2-phenyl-1-propanol (2P1P) were considered. These substrates are commonly used in transesterification reactions with vinyl butyrate carried out by serine proteases in nonaqueous solvents. The availability of experimental data for this reaction using cutinase in acetonitrile (40) and supercritical CO_2 (41) has prompted this choice. The model compound modeled in the enzyme active site was the second TI in the reaction mechanism of transesterification of *sec*-alcohols catalyzed by serine proteases (Fig. 1). This TI is thought to be the rate-limiting step in the catalytic mechanism of serine proteases (6) and has been used for characterizing kinetics assuming that it closely resembles the TS (6,42). In fact, the ab initio energy difference calculated between the TS and the corresponding TI in the mechanism of serine proteases is very small (43).

The R enantiomers of the TI from 1PE (TI-1PE) and 2P1P (TI-2P1P) were modeled in the cutinase active site based on previous cutinase-inhibitor x-ray structures (44–46). The long hydrophobic tail of vinyl butyrate was placed along the hydrophobic cleft of the active site, while the bulky phenyl ring was fitted on the opposite side. The TI was linked to the O_γ of the catalytic serine with the most negative oxygen atom of the TI facing the oxyanion hole (46). Energy minimization was applied to the position of the TI and surrounding side-chain residues: Asp-159 and His-172 of the catalytic triad; Ser-26 and Gln-105, including the NH in the oxyanion hole; Asn-68 in close contact with the butyrate tail; and Tyr-103, Leu-173, Val-168, Glu-28, and Thr-27 in close vicinity of the phenyl ring of the alcohol part. We performed 5000 steps of steepest descent energy minimization with

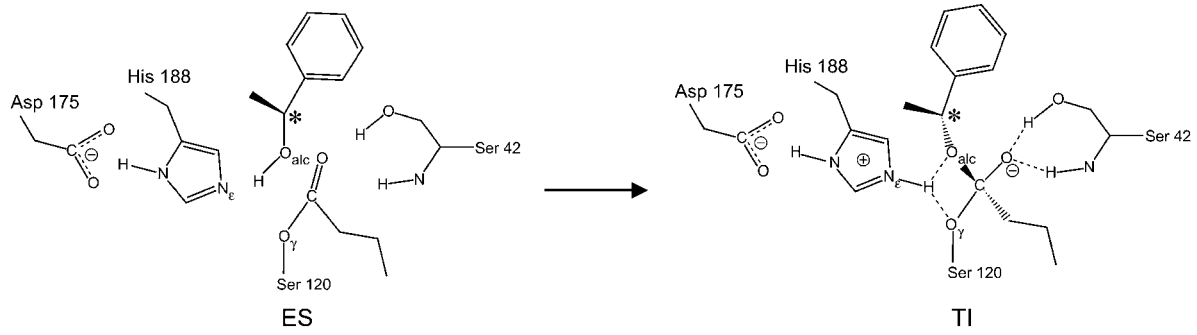

FIGURE 1 Second TI in a *sec*-alcohol transesterification reaction catalyzed by serine proteases. After the attack of vinyl butirate and the formation of the first TS, the alcohol substrate, in this case (R)-1PE, attacks the catalytic histidine and generates a second TS before the release of the ester product. The chiral center in the R conformation is marked with an asterisk. ES denotes the enzyme-substrate complex.

all atoms harmonically restrained with a force constant of 10^6 kJ mol^{-1} nm^{-1}, except for the side chains of the residues previously mentioned. The substrates' bonded and nonbonded parameters were based on the GROMOS96 force field (31). Partial charges were calculated for the model compounds of the TI (Table 1 and Fig. 2) of both substrates using the Restrained ElectroStatic Potential fit charge model (RESP) method (47) based on electrostatic potentials calculated with GAUSSIAN98 (48). These atoms belong to the TI, having a global charge of −1. Geometry optimization of the all-atom model compound was performed in the gas phase at the Hartree-Fock level, using the 6-31G(d) basis set.

Free energy calculations

The evaluation of the enantiomeric preference of cutinase with different hydration levels was assessed by considering the thermodynamic cycle in Fig. 3 (which illustrates the case of 1PE). This thermodynamic cycle evaluates the relative stability between the R to S substrate transformation in the active site and in solution, and it can be interpreted as corresponding to the following reaction:

$$\begin{aligned}\mathrm{Enzyme:Substrate(R)} + \mathrm{Substrate(S)} \\ \rightarrow \mathrm{Enzyme:Substrate(S)} \\ + \mathrm{Substrate(R)},\end{aligned} \quad (1)$$

whose relative free energy $\Delta\Delta G_{RS}$ is given by

$$\Delta\Delta G_{RS} = \Delta G_{RS} - \Delta G_{RS}^{Solvent}. \quad (2)$$

TABLE 1 Partial atomic charges (*q*) of the tetrahedral intermediates used (see Fig. 2)

	2-phenyl-1-propanol		1-phenylethanol		
Atom name	GROMOS 96 atom code	*q*	GROMOS 96 atom code	*q*	Charge source
CA	CH2	0.00000	CH2	0.00000	GROMOS
CB	CH2	0.05456	CH2	0.05456	QM/RESP
OA	OA	−0.50444	OA	−0.50444	QM/RESP
C1	C	0.99183	C	0.99183	QM/RESP
C2	CH2	−0.26773	CH2	−0.26773	QM/RESP
C3	CH2	0.00000	CH2	0.00000	GROMOS
OM	OM	−0.85436	OM	−0.85436	QM/RESP
OAP	OA	−0.46929	OA	−0.46929	QM/RESP
CP1	CH2	0.04943	CH1	0.04943	QM/RESP
CP2	CH1	0.00000	CH3	0.00000	GROMOS
CP3	CH3	0.00000	-	-	GROMOS
CG	C	0.00000	C	0.00000	GROMOS
CD1	C	−0.10000	C	−0.10000	GROMOS
HD1	HC	0.10000	HC	0.10000	GROMOS
CD2	C	−0.10000	C	−0.10000	GROMOS
HD2	HC	0.10000	HC	0.10000	GROMOS
CE1	C	−0.10000	C	−0.10000	GROMOS
HE1	HC	0.10000	HC	0.10000	GROMOS
CE2	C	−0.10000	C	−0.10000	GROMOS
HE2	HC	0.10000	HC	0.10000	GROMOS
CZ	C	−0.10000	C	−0.10000	GROMOS
HZ	HC	0.10000	HC	0.10000	GROMOS
C4	CH4	0.00000	CH4	0.00000	GROMOS

QM/RESP labels the atoms of the model compound that were set free during RESP fitting. GROMOS labels the atoms on which charges were imposed to be as the ones employed in the GROMOS force field during RESP fitting.

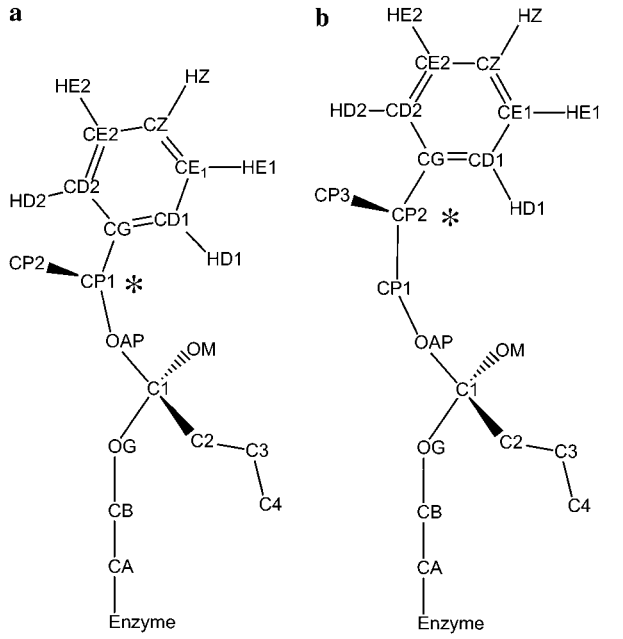

FIGURE 2 Schematic model of the TI. (*a*) (R)-1PE and (*b*) (R)-2P1P. The chiral center in the R configuration is marked with an asterisk.

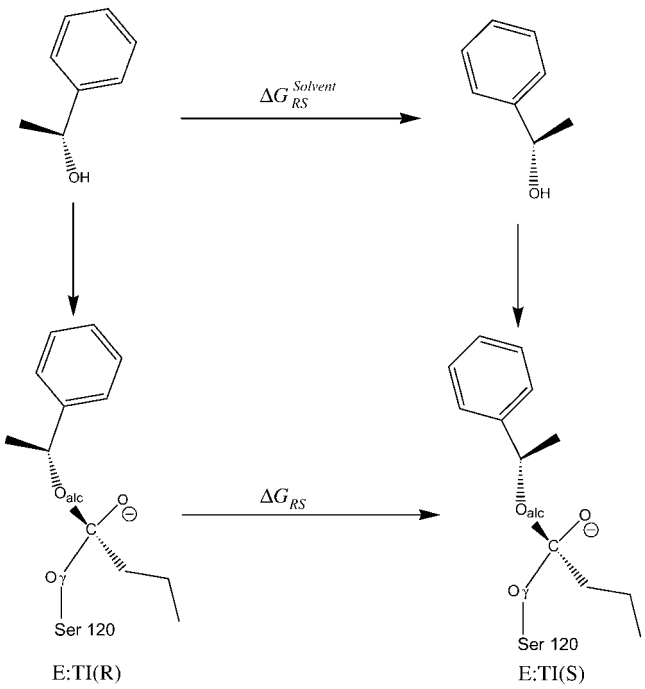

FIGURE 3 Thermodynamic cycle considered for computing the relative stability between the R and S substrates studied (exemplified for the case of 1PE) in solution and bound at the active site. ΔG_{RS} is calculated via thermodynamic integration. The E:TI(R) to E:TI(S) denotes the thermodynamic integration from R to S of the covalently bound TI at the active site of the enzyme. ΔG_1 corresponds to the special case of enantiomers in an achiral environment with equivalent ground state energies (see text).

Knowing that two enantiomers in an achiral environment have the same physical-chemical properties (49), we have that $\Delta G_{RS}^{Solvent} = 0$ kJ/mol, regardless of whether the isomerization takes place in hexane or in water, leading to

$$\Delta\Delta G_{RS} = \Delta G_{RS} \tag{3}$$

reducing our free energy calculations to the evaluation of the relative stability between the enantiomeric TI bound at the enzyme active site. The thermodynamic cycle is applied at each hydration condition, with the transformation step of the substrate in solution being equivalent for all and assuming, as usual, the same free energy of the Michaelis-Menten enzyme-substrate complex for both enantiomers. The chiral compound under study simply differs on the orientation of the methyl group attached to the chiral center (Fig. 2). This is modeled using an improper dihedral potential that determines the right chirality for the R and S compounds. This improper dihedral is changed using thermodynamic integration (50) in the ΔG_{RS} branch of the thermodynamic cycle (Fig. 3).

After 5 ns of simulation of the enzyme with the TI in the R configuration, a thermodynamic integration with 11 equally spaced sampling points was used to go from the R conformer to the S conformer, according to (50).

$$\Delta G = \int_0^1 d\lambda \left\langle \frac{\partial H(\lambda)}{\partial \lambda} \right\rangle_\lambda . \tag{4}$$

Each λ step was 50 ps long, with 10 ps used for equilibration and 40 ps used for productive sampling. To slowly change from one λ step to the next one, a nonproductive 10 ps slow growth method was used.

RESULTS AND DISCUSSION

The dependence of the enzyme enantioselective properties on the amount of water present in nonaqueous solvents was motivated by our previous analysis of the structural and dynamical properties of cutinase in hexane (26). It was found that the structural and dynamical properties of the enzyme at 5–10% (w/w) water content are similar to what is found in water simulations. In the water range studied, from 0% to 25% water content, it was noticed that at 0% and 2.5% the enzyme structure is extremely rigid, and higher water levels over 25% would lead to a complete destruction of the enzyme. The implications of the computer simulations with very low percentages of water in the assessment of further conclusions are not trivial. In practice, the total removal of water from the structure implies that the internal waters known to be structurally essential are not present. Furthermore, extensive drying experiments of enzymes have shown the inability of removing these internal waters (51). There are diverse estimates of the minimum amount of water necessary for catalysis (52). In hydrated enzyme powders a threshold value of 20% (w/w) water is generally accepted, whereas in nonaqueous systems it is known that enzyme activity is possible at lower hydration levels (52). The total or partial removal of the internal waters of the enzyme crystal and the replacement of the aqueous solvent by a very low dielectric media, such as hexane, will restrain and kinetically trap the system at the starting configuration. In free energy calculations by MD simulations this artifact is of major concern since a proper sampling of the accessible configurational

space should be ensured. In our study we assumed a minimum amount of water of 5% (w/w), corresponding to 57 water molecules, similar to the number of the less accessible water molecules present in the cutinase crystal.

Enzyme enantioselectivity prediction

The free energy ΔG_{RS} computed for the TI of each substrate, 1PE and 2P1P, is shown in Fig. 4 for five different solvation environments (5%, 7.5%, 10%, 15%, 25%). This free energy measures the relative stability of the R and S enantiomers of the TI in the active site. These results indicate that for both chiral substrates bound at the enzyme active site, the equilibrium is favored toward the R enantiomer. Furthermore, it shows that the R enantiomer of 1PE is more stabilized than the R enantiomer of 2P1P at all water percentages. Experimentally, the 1PE substrate was used in supercritical CO_2 with cutinase immobilized onto a zeolite support (41). It was shown that the enzyme catalytic activity was dependent on the water content, with exclusive preference toward the R enantiomer in the range of a_w tested. The 2P1P was recently employed in the transesterification reaction by cutinase in acetonitrile at different water activities and immobilization supports (40). The resolution of this substrate was low but still with a preference toward the R enantiomer. These experimental evidences for both substrates are predicted by our study: first, in both experiments where 1PE and 2P1P have been employed, it is the R enantiomer that is more stabilized by the enzyme as has been shown by our calculations; and second, for both substrates, the enantiomeric discrimination is higher in magnitude for (R)-1PE in comparison to (R)-2P1P. It can be seen that not only can it be predicted which is the better stabilized enantiomer in the cutinase active site, but also, using two different substrates with equivalent chiral properties, it is possible to evaluate the magnitude of the preferred ones.

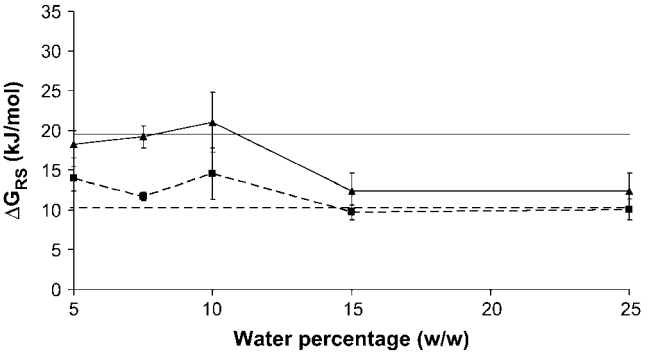

FIGURE 4 Free energy difference, ΔG_{RS} (Fig. 3), between the R and S TI of 1PE (*triangles* with *solid line*) and 2P1P (*squares* with *dashed line*), bound at the active site of cutinase solvated in hexane with ions and increasing amounts of water. The horizontal solid and dashed lines represent ΔG_{RS} for 1PE and 2P1P, respectively, bound to the enzyme in pure water. Relative free energies are calculated based on the average of five thermodynamic integration replicates for each hydration condition in hexane and three replicates for the pure water simulations (see Material and Methods). Error bars are estimated from the standard error of the five replicate values.

Correlation between ΔG_{RS} and hydration

The free energy difference between the R and S enantiomers of both TI substrates shows an interesting dependence on the amount of water present (Fig. 4). It is possible to observe a maximum of the free energy of stabilization up to 21.0 kJ/mol of the R enantiomer relative to the S enantiomer at 10% water content for 1PE, followed by a significant decrease at higher water percentages. On the other hand, the free energy for 2P1P is not so affected in the water range tested, but a maximum can be found in the low water range at 10%. For both substrates, the stabilization of the TI is maximized at 10% water range. This evidence suggests that the enzyme structural and dynamical properties that are found to be more nativelike in the 5–10% water range also provide the conditions to maximize the enantioselective properties of the enzyme. This evidence qualitatively agrees with the experimental results of the water effect on the enantioselective properties of some enzymes in nonaqueous solvents previously discussed in the Introduction. It shows that the catalytic properties concerning the discriminative power of the enzyme are under the control of the structural and dynamical properties of the whole enzyme, which are, in turn, modeled by the different hydration levels in hexane.

Correlation with structural properties

The previous results prompt us to look for the structural and electrostatic properties of the enzyme that account for the ΔG_{RS} observations at the different hydration levels. It is commonly assumed that the three-dimensional structures of the proteins are correlated with their function and, in the case of enzymes, with their ability to perform as catalysts. The 5–10% range of water content, where the structural and dynamical properties of cutinase resemble the water simulations (26), is also the range where our calculations estimate enantioselectivities of the R enantiomers of both substrates to be the highest. The loss of structural integrity at high water percentages, observed as an increase of the rms deviation from the x-ray structure (26), correlates with a decrease in the ability of the enzyme to discriminate the enantiomers (Fig. 4). However, the overall rms deviation of the structure does not capture the small details occurring at the active site, neither does it explain how the global conformational changes are transferred to the active site. The rms deviation of the surrounding residues of the active site, including the catalytic triad, is quite low along the water range, with a significant increase found at 25% and only for the case of 1PE (Fig. 5 *a*). The high stability of the active site may rely, as known, on the nature of the enzyme folding in keeping these residues at their relative positions. Therefore, in this water range, the changes in the overall structure do not imply

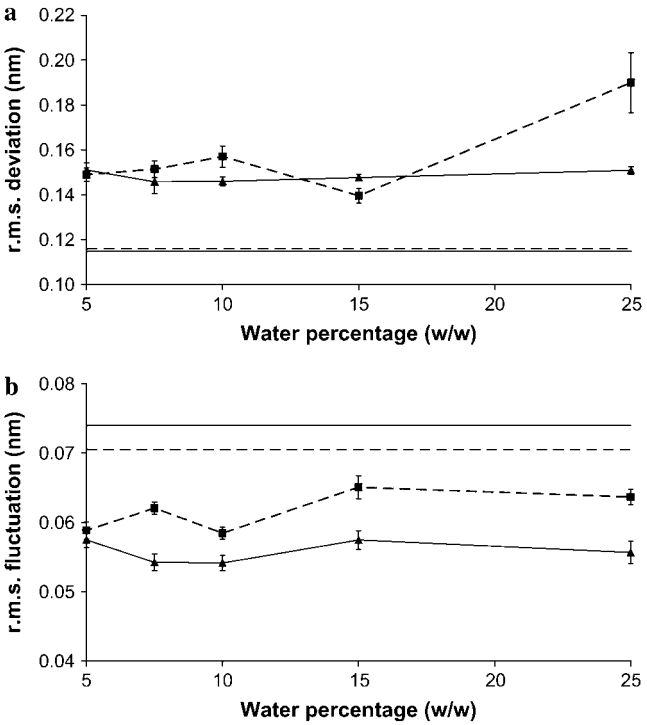

FIGURE 5 Structural analysis of the cutinase active site. The active site residues considered are the ones located in close contact with the TI. Side chains of the residues included are Gly-41, Ser-41 (oxianion hole), Gln-121 (including the NH involved in the oxianion hole), Glu-44, Tyr-109, Ser-120 (catalytic serine up to the Oγ oxygen), Asp-175 (of the catalytic triad), Val-184, His-188 (of the catalytic triad), and Leu-189. The solid line corresponds to the system with the TI from (R)-1PE, and the dashed line to the system with the TI from (R)-2P1P. The horizontal solid and dashed lines represent data from cutinase simulations in pure water with (R)-1PE and (R)-2P1P, respectively. (*a*) rms deviation of the active site residues considered fitted against the x-ray structure for the different amounts of water tested. (*b*) rms fluctuation of the active site residues considered for the different amounts of water tested. Values and error bars are calculated on the basis of the average of five replicates for each hydration condition.

a significant loss of the structural properties of the active site residues. On the other hand, the dynamical behavior of the residues located at the active site can be, to some extent, correlated with the amount of water present (Fig. 5 *b*). The data show a minimum of the rms fluctuation of the residues at the active site (excluding the TI) within the low water range 5–10%. The rms fluctuation of these residues increases at higher water percentages (15–25%). Another point is the fact that the rms fluctuation of the active site residues of the enzyme that interact with the (R)-2P1P TI, which has a larger alcohol substrate, is systematically higher than with the smaller alcohol substrate, (R)-1PE. This difference can be attributed to the structural properties of the substrates, given that the (R)-1PE alcohol part of the TI is well buried in the active site, whereas the longer (R)-2P1P part of the TI is more exposed to the solvent, being less constrained by the active site residues, and affecting the flexibility of these residues. An average structure of the active site with both R and S enantiomers from a representative MD run at 10% (w/w) illustrates this description (Fig. 6). It shows that, for the TI-1PE, both R and S enantiomers are restrained and deeply buried at the active site. However, for the R and S enantiomers of TI-2P1P, the phenyl ring is pointing out of the active site and less constrained by the neighboring residues and more exposed to the solvent (40).

Correlation with the catalytic His

A more specific structural description of the stability and configuration of the TI enantiomers arises from the hydrogen bond pattern between the catalytic histidine and the TI bound at the active site. It has been previously reported that in the catalytic mechanism of serine protease in the transesterification of *sec*-alcohols, the faster reacting enantiomer could be successfully correlated with the persistence of the hydrogen bond between the N_ε from the catalytic histidine and the O_{alc} from the alcohol group (24,53,54). These authors suggest that the weakening or total loss of the $N_\varepsilon - O_{alc}$ hydrogen bond determines the slow reaction enantiomer, whereas the persistence of this hydrogen bond interaction is responsible for the faster reacting one. The frequency of the $N_\varepsilon - O_{alc}$ hydrogen bond for each enantiomer is analyzed in Fig. 7, showing a qualitative agreement with the experimental results. In the TI of 1PE, this hydrogen bond in the R configuration is very frequent, whereas in the S configuration it is very rare or absent (Fig. 7 *a*). The basis of the exclusive preference observed experimentally for the R enantiomer can be correlated with this hydrogen bond property. The frequency of this hydrogen bond in the TI of (R)-1PE also seems to be affected by the amount of water in the media. In the low water range, the R enantiomer has maxima for the $N_\varepsilon - O_{alc}$ hydrogen bond at 7.5% and 15%, although the data is not clear concerning the point with 10% water content and this may reflect the competition of the Oγ of the catalytic serine for the N_ε. This hydrogen bond is important for the histidine attack and release of the product. At high percentages of water (25%), the frequency of the $N_\varepsilon - O_{alc}$ hydrogen bond seems to be affected by the structural changes occurring in the enzyme, thus affecting the stabilization of the (R)-1PE TI. The structural basis for the productive orientation of the O_{alc} is closely related to the configuration of the chiral center. The R configuration of the alcohol substrate provides a proper orientation of the O_{alc} toward the N_ε of the catalytic histidine, whereas the S conformation imposes a displacement of the O_{alc} in the opposite way, breaking the hydrogen bond with N_ε. For the 2P1P substrate, an extra CH_2 group lies between the chiral center and the O_{alc}, implying that the steric effects in changing the chirality from R to S do not affect to a great extent the orientation of the O_{alc} atom, and thus the stabilizing hydrogen bond. This property is reflected on the hydrogen bond frequency observed for both R and S enantiomers of the 2P1P TI (Fig. 7 *b*), which show

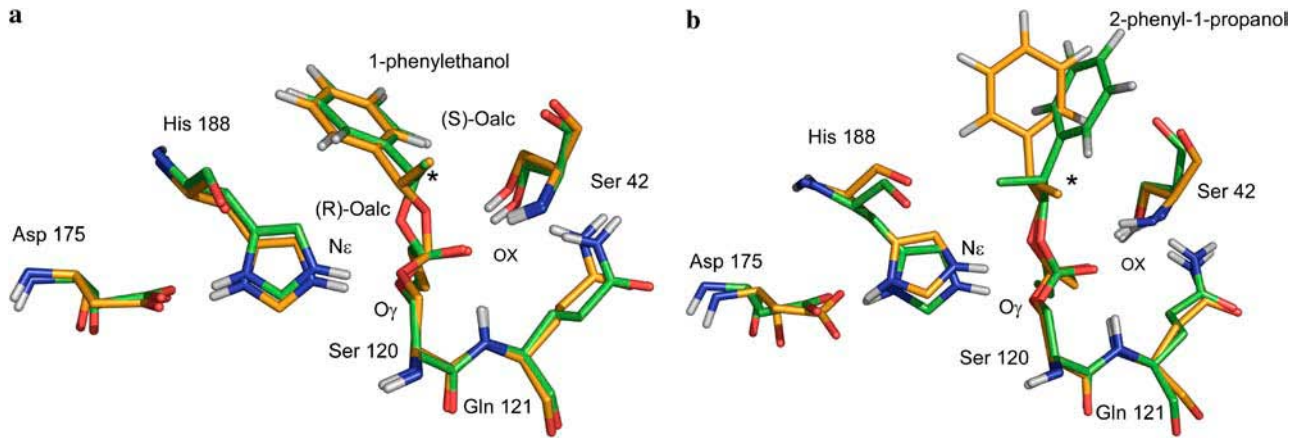

FIGURE 6 TI under study bound at the cutinase active site. Active site residues considered are Asp-175, His-188, Ser-120, Gln-121, and Ser-42. OX labels the oxianion hole formed by the NH of Gln-121 and Ser-42. The chiral center is marked with an asterisk. (*a*) Overlap of the R (*green* carbons) and S (*orange* carbons) 1PE TI average structure from MD simulations (3–7 ns) in hexane with ions and 10% (w/w) water content. (*b*) Overlap of the R (*green* carbons) and S (*orange* carbons) 2P1P TI average structure from MD simulations (3–7 ns) in hexane with ions and 10% (w/w) water content.

statistically equivalent hydrogen bond frequencies for each water percentage, except for 15% of water content. However, for 2P1P, this hydrogen bond does not provide an explanation for the preferential stabilization, although lower, of the R enantiomer. As for 1PE, the magnitude of the decreasing trend is observed for water percentages higher than 15%. This analysis shows that the frequency of this important hydrogen bond can be affected by small localized structural and dynamical changes at the catalytic active site.

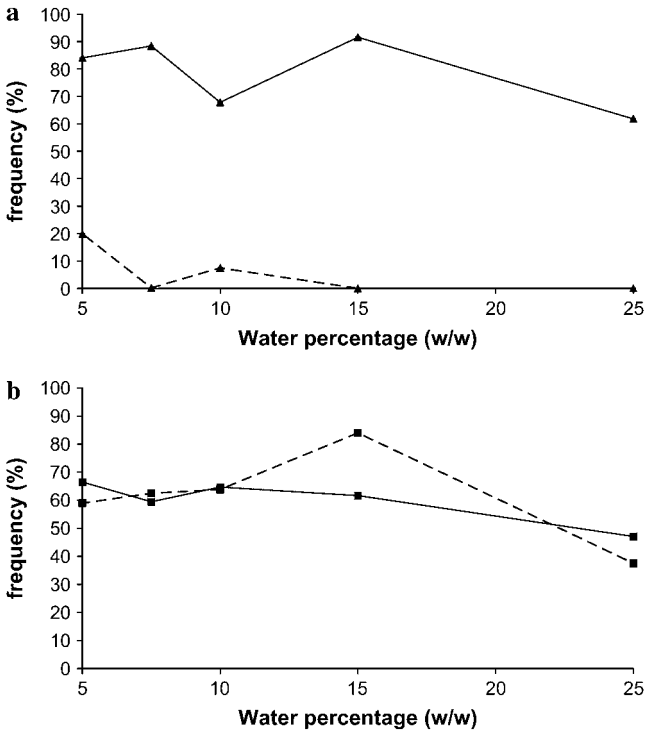

FIGURE 7 $N_{\varepsilon} - O_{alc}$ hydrogen bond frequency of the R and S TI enantiomers. (*a*) 1PE and (*b*) 2P1P. Solid line marks the R enantiomer and the dashed line the S enantiomer. Frequencies are estimated from 500 ps before the thermodynamic integration for the R enantiomer and 500 ps after the thermodynamic integration for the S enantiomer. Averages and error bars are calculated based on five replicates for each hydration condition.

Nonbonded effects

On the basis that enzymes operate by stabilizing the TSs through electrostatic complementary of the active site, by means of predefined dipoles (6), we evaluate this effect through the analysis of the nonbonded interactions (van der Waals and Coulomb) of the protein residues on the R and S TI of both substrates. Our approach is focused on the role of the large stabilization effect of the TI by the catalytic histidine (6) present in the serine proteases' active site architecture. These effects are incorporated in part in the previous results on the hydrogen bond between the catalytic histidine and the TI. The perturbation of this electrostatic stabilization due to conformational changes of the enzyme imposed by the molecular composition of the solvent might be in part responsible for the differences in the ΔG_{RS} calculated (Fig. 4). It is observed that the catalytic histidine is responsible for a large energetic stabilization effect on the TI of (R)-1PE (Fig. 8 *a*), and the S conformation is much less stabilized. The difference of this nonbonded stabilizing effect of the R and S enantiomers of the 1PE TI (Fig. 8 *c*) reveals a high stabilization of the R conformer relative to the S at the 10% water content, followed by a decreasing of stabilization for high and low water percentages. For the R and S TI enantiomers of 2P1P, the difference of the stabilization energy provided by the catalytic histidine between the R and S conformers is small (Fig. 8 *b*), indicating that both TIs are stabilized by the same magnitude, with a small

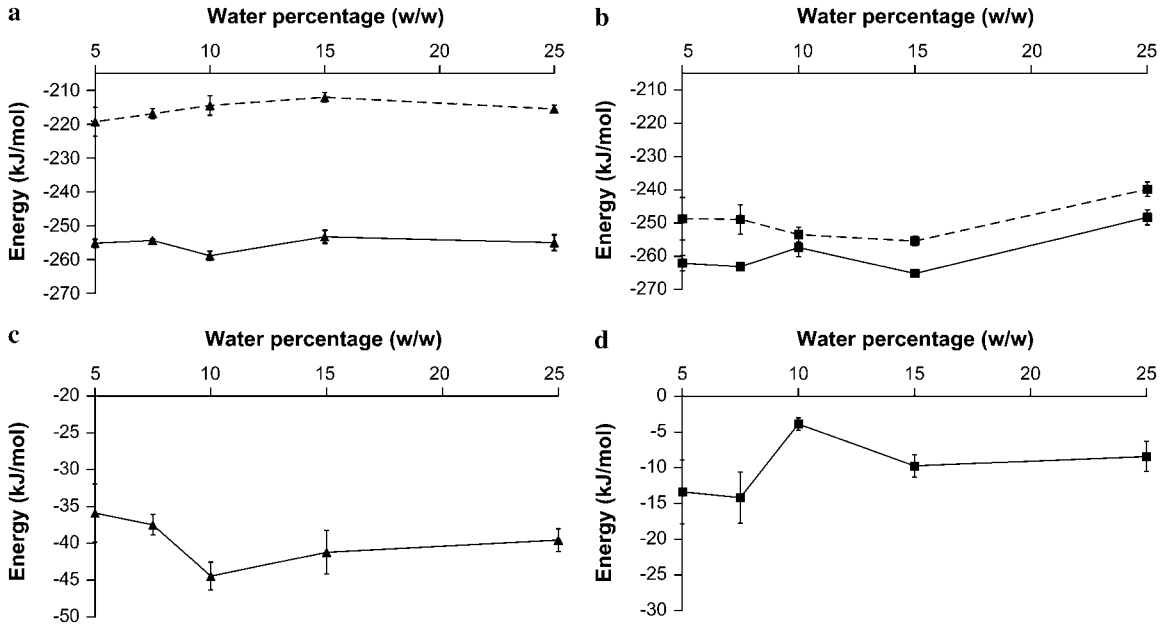

FIGURE 8 van der Waals plus Coulomb interactions of the catalytic His-188 with the TI. (*a*) R enantiomer (*solid line*) and S enantiomer (*dashed line*) of the TI of 1PE. (*b*) R enantiomer (*solid line*) and S enantiomer (*dashed line*) of the TI of 2P1P. (*c*) Energy difference (R − S) of the interaction energy between the catalytic His-188 and the R and S TI of 1PE shown in *a*. (*d*) Energy difference of the interaction energy between the catalytic His-188 and the R and S TI of 2P1P shown in *b*. Values and error bars are calculated based on the average of five replicates for each hydration condition.

preference for the R enantiomer. The relative stabilization between the R and S provided by the histidine also shows a higher effect at low water content (5–7.5%) that is mainly due to a decrease in the stabilization of the S enantiomer (Fig. 8 *d*). At higher water percentages both enantiomers are less stabilized by the histidine.

This particular analysis points in the same direction as the initial analysis made from the free energy calculation. Both approaches predict which enantiomer is better stabilized for both substrates, but they also indicate the difference in magnitude between the same enantiomeric substrates, (R)-1PE and (R)-2P1P. This suggests that most of the enantioselective properties of the enzyme might be located in the electrostatic and van der Waals interactions between the catalytic histidine and the TI.

CONCLUDING REMARKS

Although nonaqueous enzymology has provided many advances in the fundamental and applied use of enzymes in nonaqueous media, a detailed molecular description of the major catalytic phenomena in such media is still to be fully provided. We show, by means of free energy calculations, that the enantioselectivity of the enzyme toward two enantiomeric substrates can be predicted, as well as the extent of the preferential stabilization of the 1PE and 2P1P R enantiomers. More important, the control that water exerts on the enantioselective properties of the enzyme has been shown. As has been extensively reported, one of the key factors that control enzyme enantioselectivity in nonaqueous media is the amount of water present in the media. Our work describes these phenomena by showing that the preferential stabilization of the R enantiomer is located in the 5–10% water range where the structural and dynamical properties of cutinase are more nativelike. Besides the high reliability of our modeling studies in predicting the well-known enantioselective properties of the enzyme, we provide structural and energetic determinants that are correlated with our observations. We show that the R enantiomer substrates inside the enzyme active site provide the proper orientation for the nonbonded interaction between the catalytic histidine and the TI, and this fact determines the specificity of the enzyme toward R enantiomers. It is also described how the effect of different hydration levels on the global structure of the enzyme are able to interfere with the enantioselective properties of the enzyme, showing that the stabilizing effect of the catalytic histidine are maximized in a specific water range (5–10%). These results thus provide valuable insight into the study and design of enantiomeric substrates in the framework of enzyme enantioselectivity and dependence on hydration conditions.

The authors acknowledge helpful discussions with Prof. Susana Barreiros and Nuno Vidinha.

The authors acknowledge the financial support from Fundação para a Ciência e a Tecnologia, Portugal, through grants PRAXIS/P/BIO/14314/1998, SFRH/BD/6477/2001, and SFRH/BD/10611/2002.

REFERENCES

1. Klibanov, A. M. 2001. Improving enzymes by using them in organic solvents. *Nature*. 409:241–245.
2. Zaks, A., and A. M. Klibanov. 1985. Enzyme-catalyzed processes in organic solvents. *Proc. Natl. Acad. Sci. USA*. 82:3192–3196.
3. Zaks, A., and A. M. Klibanov. 1988. Enzymatic catalysis in non-aqueous solvents. *J. Biol. Inorg. Chem*. 263:3194–3201.
4. Zaks, A., and A. M. Klibanov. 1988. The effect of water on enzyme action in organic media. *J. Biol. Inorg. Chem.* 263:8017–8021.
5. Valivety, R. H., P. J. Halling, and A. R. Macrae. 1992. Reaction rate with suspended lipase catalyst shows similar dependence on water activity in different organic solvents. *Biochim. Biophys. Acta*. 1118: 218–222.
6. Warshel, A., G. Naray-Szabo, F. Sussman, and J. K. Hwang. 1989. How do serine proteases really work? *Biochemistry*. 28:3629–3637.
7. Kollman, P. A., B. Kuhn, and M. Perakyla. 2002. Computational studies of enzyme-catalyzed reactions: Where are we in predicting mechanisms and in understanding the nature of enzyme catalysis? *J. Phys. Chem*. 106:1537–1542.
8. Warshel, A., F. Sussman, and J. K. Hwang. 1988. Evaluation of catalytic free-energies in genetically modified proteins. *J. Mol. Biol.* 201:139–159.
9. Cleland, W. W., P. A. Frey, and J. A. Gerlt. 1998. The low barrier hydrogen bond in enzymatic catalysis. *J. Biol. Inorg. Chem.* 273: 25529–25532.
10. Cannon, W. R., and S. J. Benkovic. 1998. Solvation, reorganization energy, and biological catalysis. *J. Biol. Inorg. Chem.* 273:26257–26260.
11. Warshel, A. 1998. Electrostatic origin of the catalytic power of enzymes and the role of preorganized active sites. *J. Biol. Inorg. Chem.* 273:27035–27038.
12. Secundo, F., S. Riva, and G. Carrea. 1992. Effects of medium and of reaction conditions on the enantioselectivity of lipases in organic-solvents and possible rationales. *Tetrahedron Asymmetry*. 3:267–280.
13. Nakamura, K., Y. Takebe, T. Kitayama, and A. Ohno. 1991. Effect of solvent structure of enantioselectivity of lipase-catalyzed transesterification. *Tetrahedron Lett*. 32:4941–4944.
14. Hirose, Y., K. Kariya, I. Sasaki, Y. Kurono, H. Ebiike, and K. Achiwa. 1992. Drastic solvent effect on lipase-catalyzed enantioselective hydrolysis of prochiral 1,4-dihydropyridines. *Tetrahedron Lett*. 33:7157–7160.
15. Fitzpatrick, P. A., and A. M. Klibanov. 1991. How can the solvent affect enzyme enantioselectivity. *J. Am. Chem. Soc*. 113:3166–3171.
16. Wescott, C. R., H. Noritomi, and A. M. Klibanov. 1996. Rational control of enzymatic enantioselectivity through solvation thermodynamics. *J. Am. Chem. Soc*. 118:10365–10370.
17. Ke, T., C. R. Wescott, and A. M. Klibanov. 1996. Prediction of the solvent dependence of enzymatic prochiral selectivity by means of structure-based thermodynamic calculations. *J. Am. Chem. Soc*. 118: 3366–3374.
18. Pepin, P., and R. Lortie. 2001. Influence of water activity on the enantioselective esterification of (R,S)-ibuprofen by crosslinked crystals of *Candida antarctica* lipase B in organic solvent media. *Biotechnol. Bioeng*. 75:559–562.
19. Persson, M., D. Costes, E. Wehtje, and P. Adlercreutz. 2002. Effects of solvent, water activity and temperature on lipase and hydroxynitrile lyase enantioselectivity. *Enzyme Microb. Technol.* 30:916–923.
20. Detar, D. F. 1981. Computation of enzyme-substrate specificity. *Biochemistry*. 20:1730–1743.
21. Wipff, G., A. Dearing, P. K. Weiner, J. M. Blaney, and P. A. Kollman. 1983. Molecular mechanics studies of enzyme-substrate interactions—the interaction of L-N-acetyltryptophanamide and D-N-acetyltryptophanamide with alpha-chymotrypsin. *J. Am. Chem. Soc*. 105:997–1005.
22. Ke, T., B. Tidor, and A. M. Klibanov. 1998. Molecular-modeling calculations of enzymatic enantioselectivity taking hydration into account. *Biotechnol. Bioeng*. 57:741–746.
23. Haeffner, F., T. Norin, and K. Hult. 1998. Molecular modeling of the enantioselectivity in lipase-catalyzed transesterification reactions. *Biophys. J*. 74:1251–1262.
24. Raza, S., L. Fransson, and K. Hult. 2001. Enantioselectivity in *Candida antarctica* lipase B: a molecular dynamics study. *Protein Sci*. 10:329–338.
25. Colombo, G., S. Toba, and K. M. Merz. 1999. Rationalization of the enantioselectivity of subtilisin in DMF. *J. Am. Chem. Soc*. 121:3486–3493.
26. Soares, C. M., V. H. Teixeira, and A. M. Baptista. 2003. Protein structure and dynamics in nonaqueous solvents: insights from molecular dynamics simulation studies. *Biophys. J*. 84:1628–1641.
27. Longhi, S., M. Czjzek, V. Lamzin, A. Nicolas, and C. Cambillau. 1997. Atomic resolution (1.0 angstrom) crystal structure of *Fusarium solani* cutinase: stereochemical analysis. *J. Mol. Biol*. 268:779–799.
28. Baptista, A. M., and C. M. Soares. 2001. Some theoretical and computational aspects of the inclusion of proton isomerism in the protonation equilibrium of proteins. *J. Phys. Chem. B*. 105: 293–309.
29. Berendsen, H. J. C., D. van der Spoel, and R. van Drunen. 1995. GROMACS—a message-passing parallel molecular-dynamics implementation. *Comput. Phys. Commun*. 91:43–56.
30. Lindahl, E., B. Hess, and D. van der Spoel. 2001. GROMACS 3.0: a package for molecular simulation and trajectory analysis. *J. Mol. Model*. 7:306–317.
31. Scott, W. R. P., P. H. Hunenberger, I. G. Tironi, A. E. Mark, S. R. Billeter, J. Fennen, A. E. Torda, T. Huber, P. Kruger, and W. F. van Gunsteren. 1999. The GROMOS biomolecular simulation program package. *J. Phys. Chem. A*. 103:3596–3607.
32. van Gunsteren, W. F., and H. J. C. Berendsen. 1990. Computer simulation of molecular dynamics: methodology, applications, and perspectives in chemistry. *Angew. Chem. Int. Ed*. 29:992–1023.
33. Hess, B., H. Bekker, H. J. C. Berendsen, and J. G. E. M. Fraaije. 1997. LINCS: a linear constraint solver for molecular simulations. *J. Comput. Chem.* 18:1463–1472.
34. Miyamoto, S., and P. A. Kollman. 1992. SETTLE—an analytical version of the SHAKE and RATTLE algorithm for rigid water models. *J. Comput. Chem.* 13:952–962.
35. Hermans, J., H. J. C. Berendsen, W. F. van Gunsteren, and J. P. M. Postma. 1984. A consistent empirical potential for water-protein interactions. *Biopolymers*. 23:1513–1518.
36. Barker, J. A., and R. O. Watts. 1973. Monte-Carlo studies of dielectric properties of water-like models. *Mol. Phys*. 26:789–792.
37. Tironi, I. G., R. Sperb, P. E. Smith, and W. F. van Gunsteren. 1995. A generalized reaction field method for molecular-dynamics simulations. *J. Chem. Phys*. 102:5451–5459.
38. Smith, P. E., and W. F. van Gunsteren. 1994. Consistent dielectric properties of the simple point charge and extended simple point charge water models at 277 and 300 K. *J. Chem. Phys*. 100:3169–3174.
39. Berendsen, H. J. C., J. P. M. Postma, W. F. van Gunsteren, A. Dinola, and J. R. Haak. 1984. Molecular dynamics with coupling to an external bath. *J. Chem. Phys*. 81:3684–3690.
40. Vidinha, P., N. Harper, N. M. Micaelo, N. M. T. Lourengo, M. D. R. G. da Silva, J. M. S. Cabral, C. A. M. Afonso, C. M. Soares, and S. Barreiros. 2004. Effect of immobilization support, water activity, and enzyme ionization state on cutinase activity and enantioselectivity in organic media. *Biotechnol. Bioeng*. 85:442–449.
41. Fontes, N., M. C. Almeida, C. Peres, S. Garcia, J. Grave, M. R. Aires-Barros, C. M. Soares, J. M. S. Cabral, C. D. Maycock, and S. Barreiros. 1998. Cutinase activity and enantioselectivity in supercritical fluids. *Ind. Eng. Chem. Res*. 37:3189–3194.
42. Fersht, A. 1999. Structure and Mechanism in Protein Science: A Guide to Enzyme Catalysis and Protein Folding. W. H. Freeman, New York.

43. Hu, C. H., T. Brinck, and K. Hult. 1998. Ab initio and density functional theory studies of the catalytic mechanism for ester hydrolysis in serine hydrolases. *Int. J. Quantum Chem.* 69:89–103.

44. Longhi, S., A. Nicolas, L. Creveld, M. Egmond, C. T. Verrips, J. deVlieg, C. Martinez, and C. Cambillau. 1996. Dynamics of *Fusarium solani* cutinase investigated through structural comparison among different crystal forms of its variants. *Proteins.* 26:442–458.

45. Longhi, S., M. Mannesse, H. M. Verheij, G. H. DeHaas, M. Egmond, E. Knoops-Mouthuy, and C. Cambillau. 1997. Crystal structure of cutinase covalently inhibited by a triglyceride analogue. *Protein Sci.* 6:275–286.

46. Martinez, C., A. Nicolas, H. Vantilbeurgh, M. P. Egloff, C. Cudrey, R. Verger, and C. Cambillau. 1994. Cutinase, a lipolytic enzyme with a preformed oxyanion hole. *Biochemistry.* 33:83–89.

47. Bayly, C. I., P. Cieplak, W. D. Cornell, and P. A. Kollman. 1993. A well-behaved electrostatic potential based method using charge restraints for deriving atomic charges—the RESP model. *J. Phys. Chem.* 97:10269–10280.

48. Frisch, M. J., G. W. Trucks, H. B. Schlegel, G. E. Scuseria, M. A. Robb, J. R. Cheeseman, V. G. Zakrzewski, J. A. Montgomery, R. E. Stratmann, J. C. Burant, S. Dapprich, J. M. Millam, A. D. Daniels, K. N. Kudin, M. C. Strain, O. Farkas, J. Tomasi, V. Barone, M. Cossi, R. Cammi, B. Mennucci, C. Pomelli, C. Adamo, S. Clifford, J. Ochterski, G. A. Petersson, P. Y. Ayala, Q. Cui, K. Morokuma, D. K. Malick, A. D. Rabuck, K. Raghavachari, J. B. Foresman, J. Cioslowski, J. V. Ortiz, A. G. Baboul, B. B. Stefanov, G. Liu, A. Liashenko, P. Piskorz, I. Komaromi, R. Gomperts, R. L. Martin, D. J. Fox, T. Keith, M. A. Al-Laham, C. Y. Peng, A. Nanayakkara, C. Gonzalez, M. Challacombe, P. M. W. Gill, B. G. Johnson, W. Chen, M. W. Wong, J. L. Andres, M. Head-Gordon, E. S. Replogle, and J. A. Pople. 1998. Gaussian 98, Revision A.7. Gaussian, Inc., Pittsburgh, PA.

49. Morrison, R. T., and R. N. Boyd. 1986. Organic Chemistry, 4th ed. Allyn and Bacon, Boston, MA.

50. Beveridge, D. L., and F. M. Dicapua. 1989. Free-energy via molecular simulation—applications to chemical and biomolecular systems. *Annu. Rev. Biophys. Biophys. Chem.* 18:431–492.

51. Dolman, M., P. J. Halling, B. D. Moore, and S. Waldron. 1997. How dry are anhydrous enzymes? Measurement of residual and buried O-18-labeled water molecules using mass spectrometry. *Biopolymers.* 41:313–321.

52. Daniel, R. M., R. V. Dunn, J. L. Finney, and J. C. Smith. 2003. The role of dynamics in enzyme activity. *Annu. Rev. Biophys. Biomol. Struct.* 32:69–92.

53. Schulz, T., J. Pleiss, and R. D. Schmid. 2000. Stereoselectivity of *Pseudomonas cepacia* lipase toward secondary alcohols: a quantitative model. *Protein Sci.* 9:1053–1062.

54. Bocola, M., M. T. Stubbs, C. Sotriffer, B. Hauer, T. Friedrich, K. Dittrich, and G. Klebe. 2003. Structural and energetic determinants for enantiopreferences in kinetic resolution of lipases. *Protein Eng.* 16:319–322.